Dual advantages of rapid zeolite channel diffusion and Ni sites: 1Ni/L-DAl zeolite enables efficient polyolefin hydrocracking to liquid fuel

Hongyu Fu[a], Huibin Liu[a, *], Abulikemu Abulizi[a, *], Kenji Okitsu [b], Yasuaki Maeda [b], Tiezhen Ren [a], Aisha Nulahong [a], Changhai Liang [c]

a State Key Laboratory of Chemistry and Utilization of Carbon Based Energy Resources, Xinjiang University, Urumqi, 830017, Xinjiang, PR China.

b Graduate School of Sustainable System Sciences, Osaka Metropolitan University, Osaka 5998531, Japan

c Laboratory of Advanced Materials and Catalytic Engineering, School of Chemical Engineering, Dalian University of Technology, Dalian 116024, China.

*Corresponding author Tel.: +86 13639966149, Fax: +86-0991-8582078,

E-mail address: huibinl@aliyun.com*(Huibin Liu)*, aablek@163.com *(Abulikemu Abulizi)*

1.1 Synthesis of Hierarchical LSP-Z100

Desilication of LSP-Z100 A certain amount of LSP-Z100 zeolite was weighed into a beaker, and a NaOH solution (0.1 M, 33 mL aqueous solution per gram of catalyst) was added, followed by stirring at 60°C for 30 minutes. After stirring, the mixture was rapidly cooled in an ice-water bath at 0°C for 15 minutes. After filtration, the solid sample was washed until the pH≈7. Subsequently, the sample was dried overnight at 70°C. Ammonium ion exchange was carried out using the same method as described in the previous section. After drying the solid, it was calcined at 550°C for 3 hours to obtain the desilicated LSP-Z100 zeolite, denoted as L-DSi.

Dealumination of LSP-Z100 Dealumination of the LSP-Z100 zeolite sample was completed under weakly acidic conditions. A certain amount of deionized water was added to a beaker, and CO_2 (50 mL/min of flow rate) was bubbled through it for 15 minutes. Subsequently, a certain amount of LSP-Z100 zeolite was weighed and placed into the deionized water (33 mL water/g cat). The mixture was stirred at room temperature for 2 hours while continuously bubbling with CO_2. After stirring, the solid sample was filtered and washed, dried overnight, and then calcined at 550°C for 4 hours to obtain the dealuminated sample, denoted as L-DAl.

Cetyltrimethylammonium bromide (CTABr) modification 7.278 g of CTABr was weighed and added to 100 mL of a NaOH solution (0.1 M). After thorough stirring, 3 g of LSP-Z100 zeolite was added, and the mixture was stirred at 60°C for 30 minutes. After stirring, the mixture was placed in an ice-water bath for 15 minutes. After filtration and washing until the pH≈7, ammonium ion exchange was performed, followed by calcination at 550°C for 4 hours to obtain the treated sample, denoted as L-CBr.

Tetrapropylammonium bromide (TPABr) modification 5.334 g of TPABr was weighed and added to 100 mL of a NaOH solution (0.1 M). After thorough stirring, 3 g of LSP-Z100 zeolite was added, and the mixture was stirred at 60°C for 30 minutes. After stirring, the mixture was placed in an ice-water bath for 15 minutes. After filtration and washing until the pH≈7, ammonium ion exchange was performed, followed by calcination at 550°C for 4 hours to obtain the treated sample, denoted as L-

TBr.

Tetrapropylammonium hydroxide (TPAOH) modification 5.08 mL of TPAOH was added to 100 mL of a NaOH solution (0.1 M). After thorough stirring, 3 g of LSP-Z100 zeolite was added, and the mixture was stirred at 60°C for 30 minutes. After stirring, the mixture was placed in an ice-water bath for 15 minutes. After filtration and washing until the pH≈7, ammonium ion exchange was performed, followed by calcination at 550°C for 4 hours to obtain the treated sample, denoted as L-TOH.

1.2 Synthesis of 1Ni/L-DAl

A certain amount of deionized water was added to a beaker, and CO_2 was bubbled through it for 15 minutes. Nickel nitrate hexahydrate ($Ni(NO_3)_2 \cdot 6H_2O$, 98%) with different mass ratios was weighed and dissolved in the CO_2 dissolved water. Then, a certain amount of LSP-Z100 zeolite was weighed and placed into the deionized water (33 mL/g cat). The mixture was stirred at room temperature for 2 hours while continuously bubbling with CO_2. After stirring, the solid sample was dried. After drying overnight, the samples were calcined at 550°C for 4 hours to obtain nickel-loaded xNi/L-DAl catalysts (where x represents the loading amount, x = 0.5, 1, 2, 5 wt%).

Reduction of Ni The xNi/L-DAl zeolite was placed in a tube furnace and reduced at 500°C for 2 hours using a H_2/Ar gas mixture (H_2/Ar = 10%/90%). After cooling down, the final xNi/L-DAl zeolite catalyst was collected.

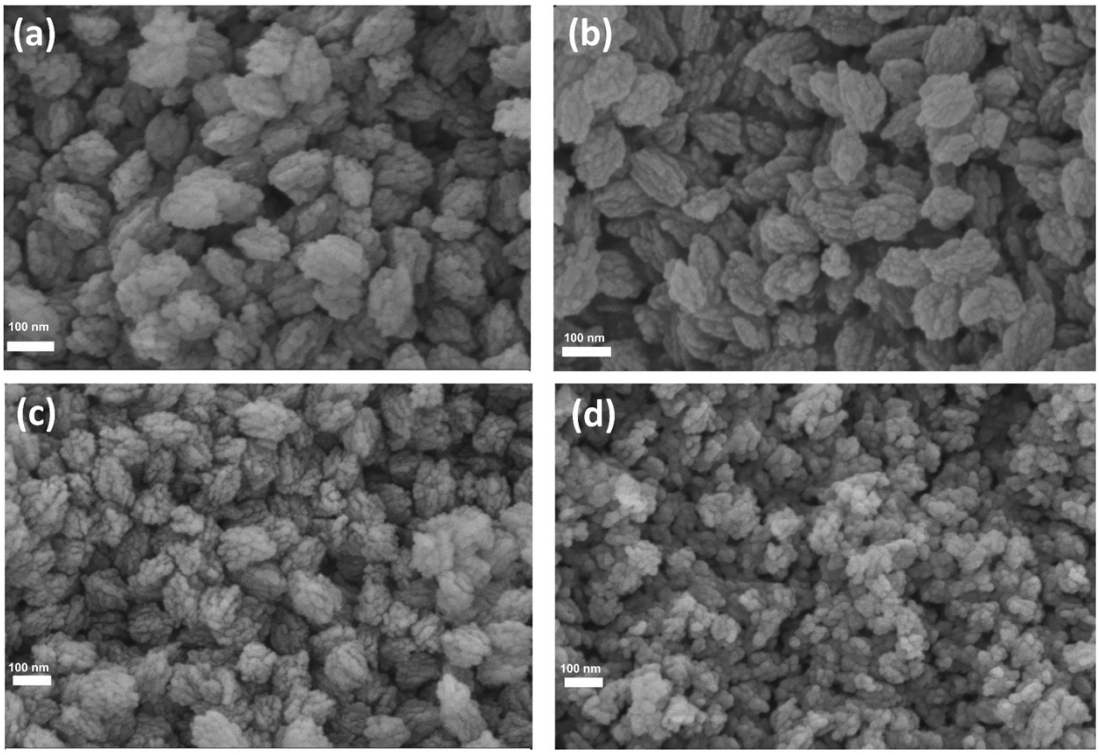

Figure S1. SEM of LSP-Z100 zeolite with different Si/Al ratios. (a) 75, (b) 100, (c) 150, (d) 200.

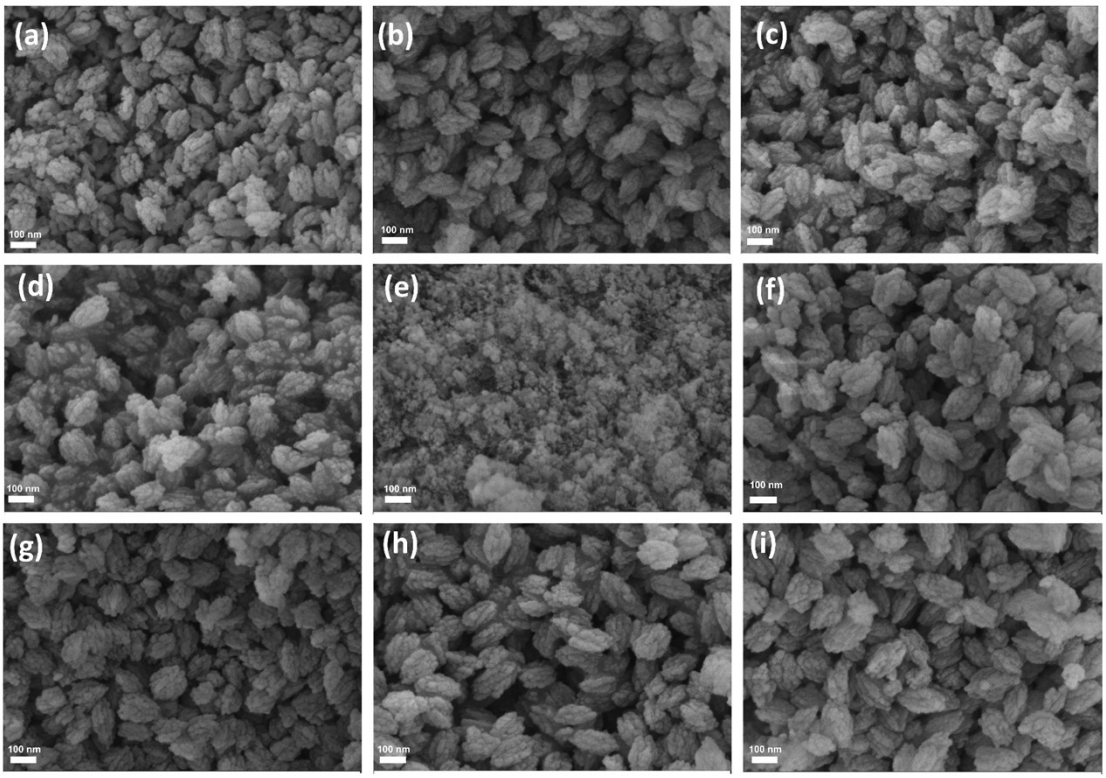

Figure S2. SEM images of LSP-Z100 zeolite treated with different modification methods (a) desilication, (b) dealumination, (c) hexadecyl trimethyl ammonium bromide (CTABr), (d) tetrapropyl ammonium bromide (TPABr), (e) tetrapropyl ammonium hydroxide (TPAOH). SEM images of LSP-Z100 zeolite loaded with different nickel metal contents after dealuminization: (f) 0.5%, (g) 1%, (h) 2%, (i) 5%.

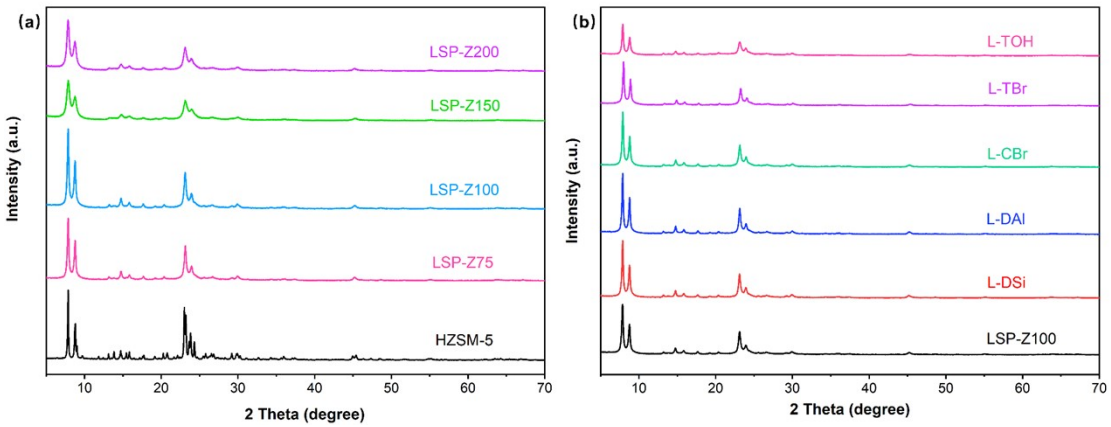

Figure S3. XRD analysis of (a) LSP zeolite with different Si/Al ratios and (b) LSP-Z100 zeolite with different modification methods

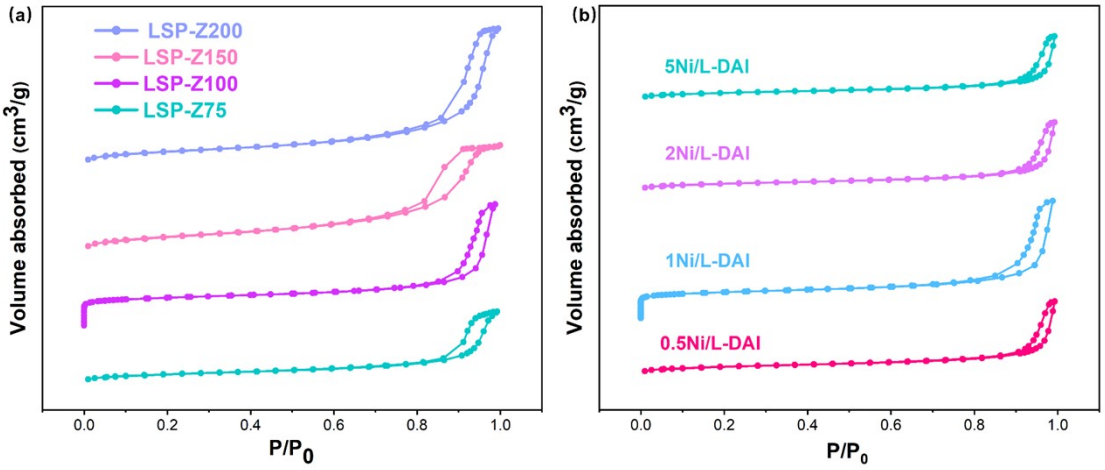

Figure S4. N_2 adsorption-desorption isotherms: (a) LSP-Z100 zeolite with varying Si/Al ratios and (b) L-DAl zeolite loaded with different Ni contents

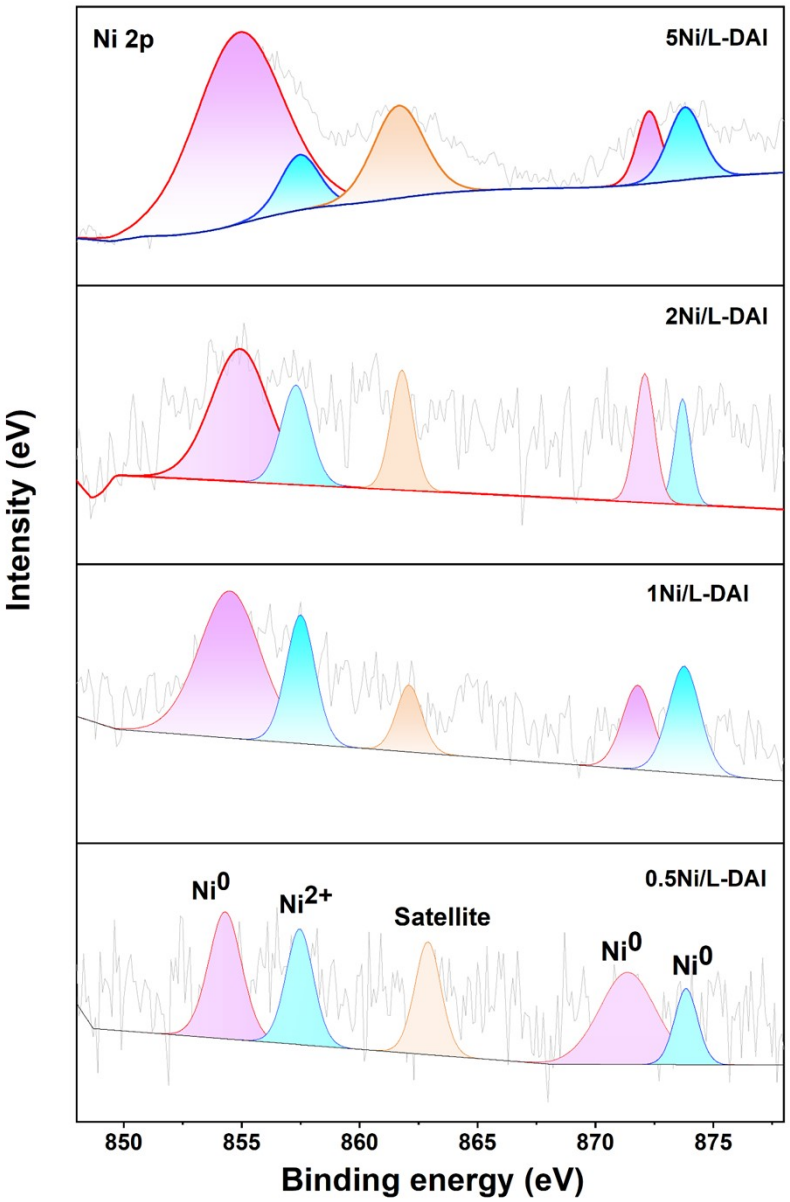

Figure S5. Ni 2p XPS spectra of L-DAl zeolites with different Ni loadings: 0.5%, 1%, 2%, 5%.

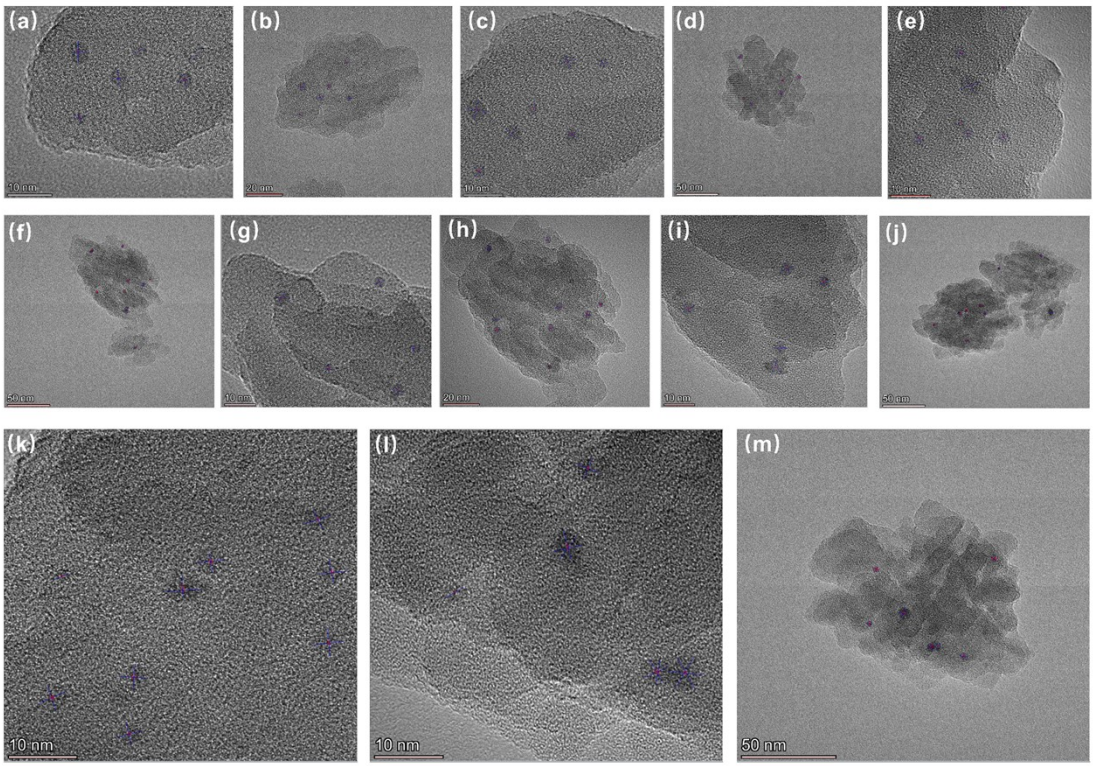

Figure S6. TEM image of the 1Ni/L-DAl catalyst with annotated dimensions of Ni atom clusters

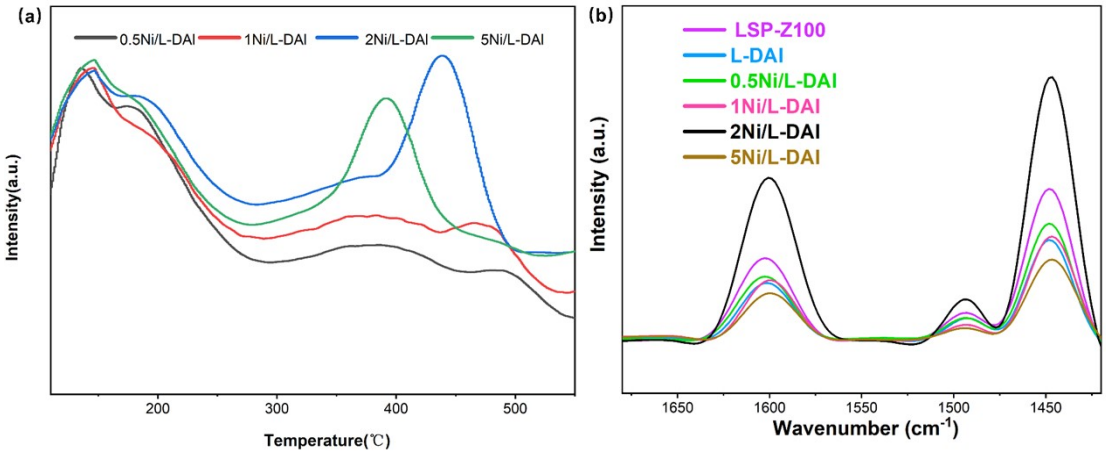

Figure S7. (a) NH_3-TPD analysis of L-DAl zeolite with different Ni loadings and (b) Py-IR analysis of LSP-Z100, L-DAl, and L-DAl with different Ni loadings

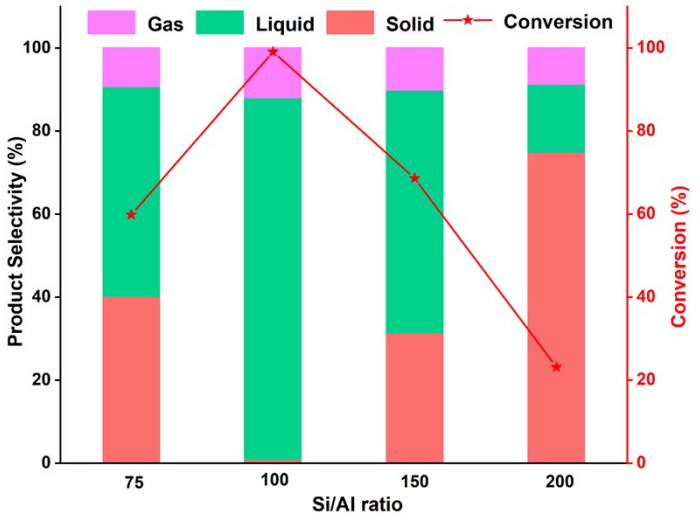

Figure S8. Hydrocracking performance of LDPE in LSP zeolites with different Si/Al ratios.

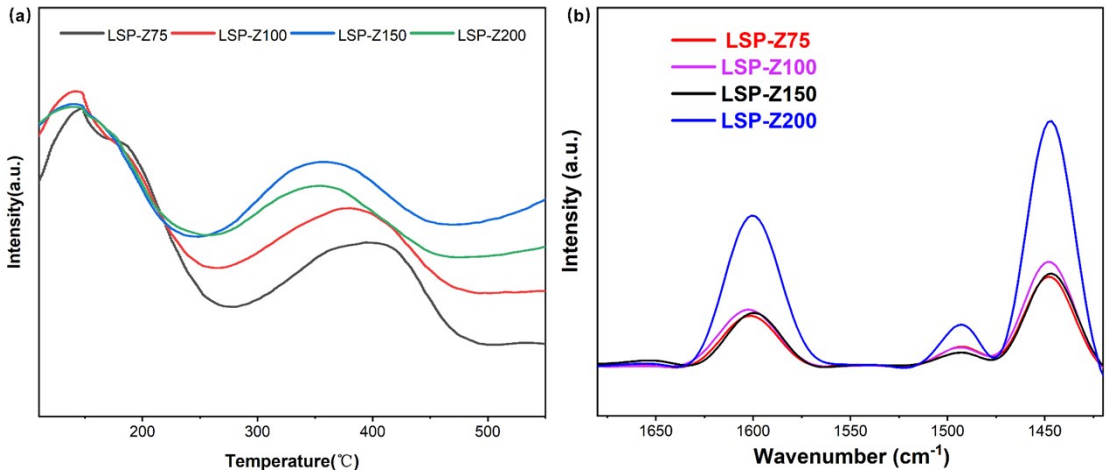

Figure S9. LSP zeolite with different Si/Al ratios: (a) NH_3-TPD analysis and (b) Py-IR analysis

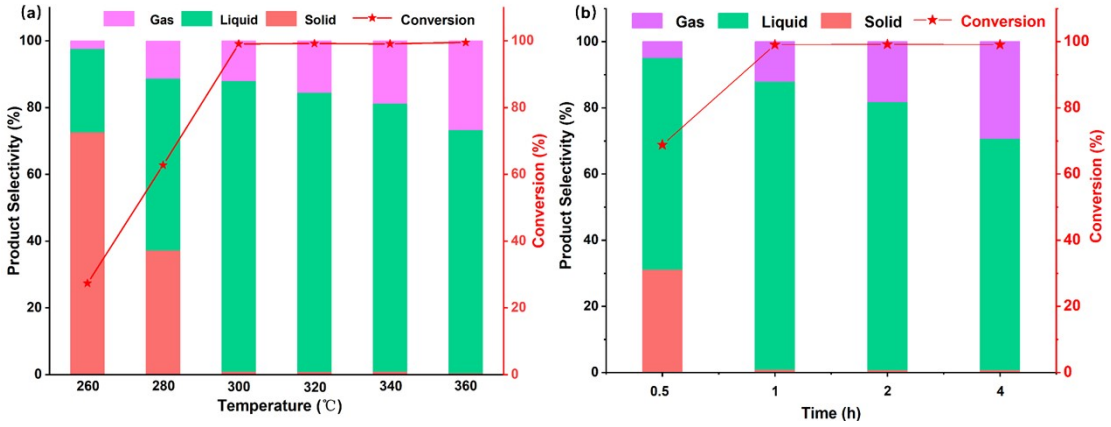

Figure S10. LDPE hydrocracking using LSP-Z100 zeolite: (a) Effect of reaction temperatures and (b) effect of reaction time

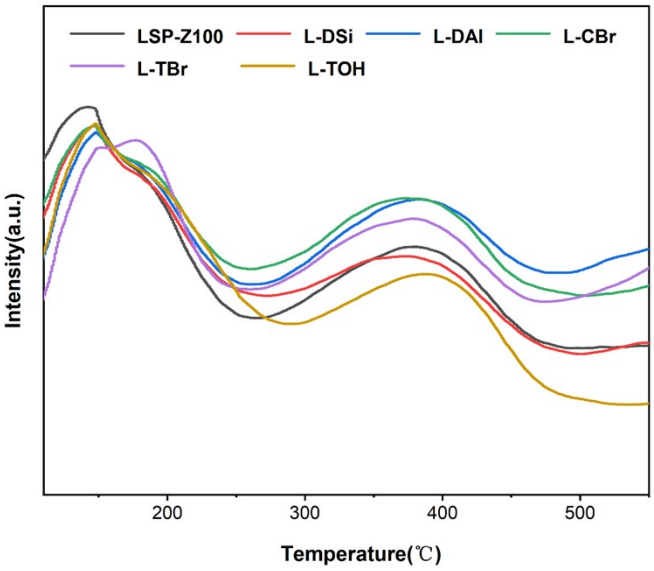

Figure S11. NH_3-TPD analysis LSP-Z100 zeolite with different modification methods.

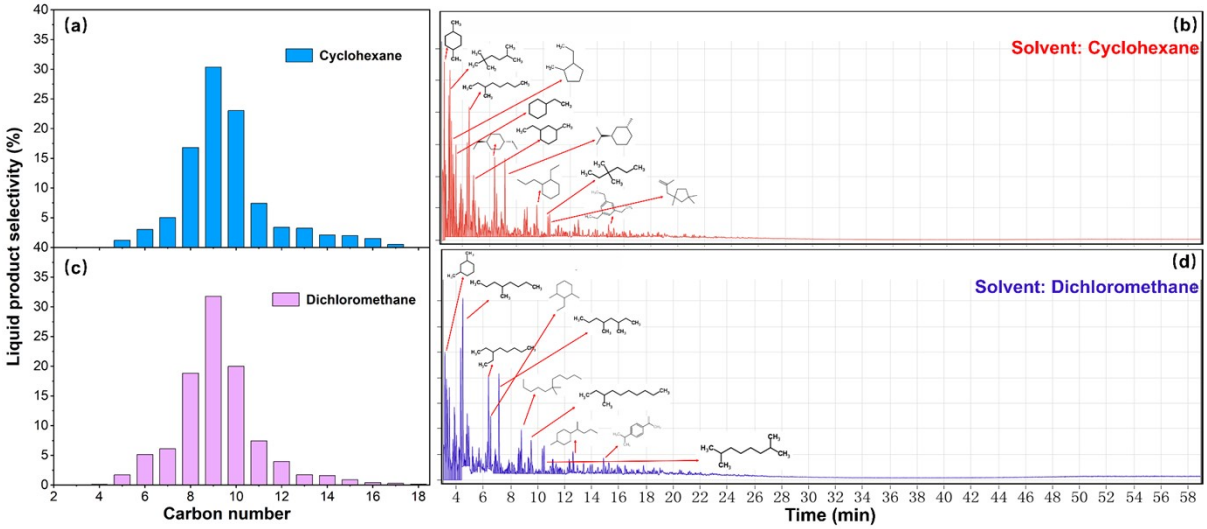

Figure S12. When hexane is used as the solvent: (a) Carbon number distribution of liquid products and (b) GC-MS analysis; When dichloromethane is used as the solvent: (c) Carbon number distribution of liquid products and (d) GC-MS analysis Reaction condition: 1Ni/L-DAl, 300°C, 1h, 2MPa of H_2.

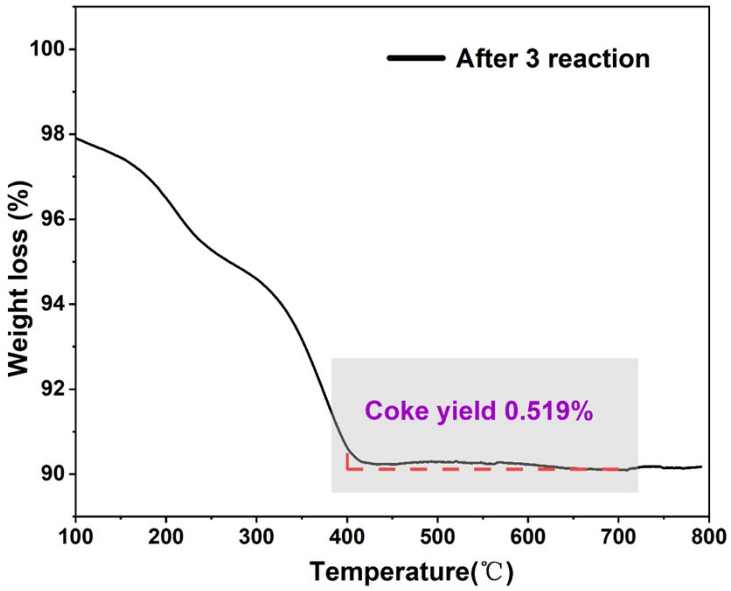

Figure S13. Thermogravimetric analysis of the 1Ni/L-DAl catalyst after three reaction cycles. Coking typically occurs between 400°C-700°C

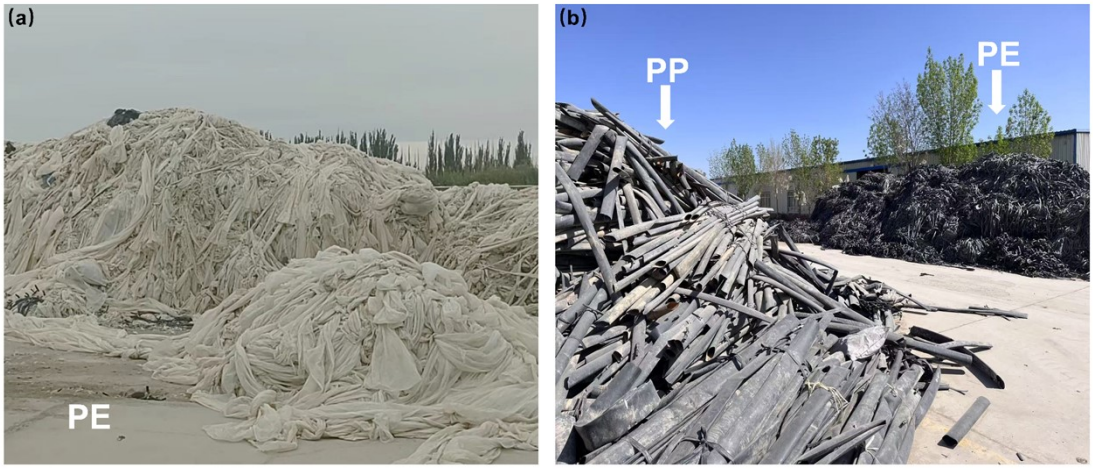

Figure S14. Plastic waste recovered from farmland in Xinjiang. (a) Used plastic mulch. (b) Drip irrigation tape

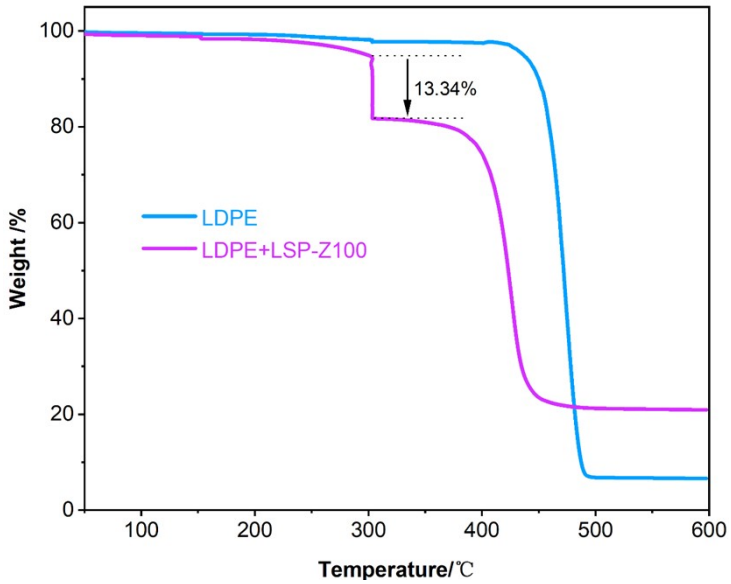

Figure S15. Segmental TGA analysis of LSP-Z100 and LSP-Z100+LDPE

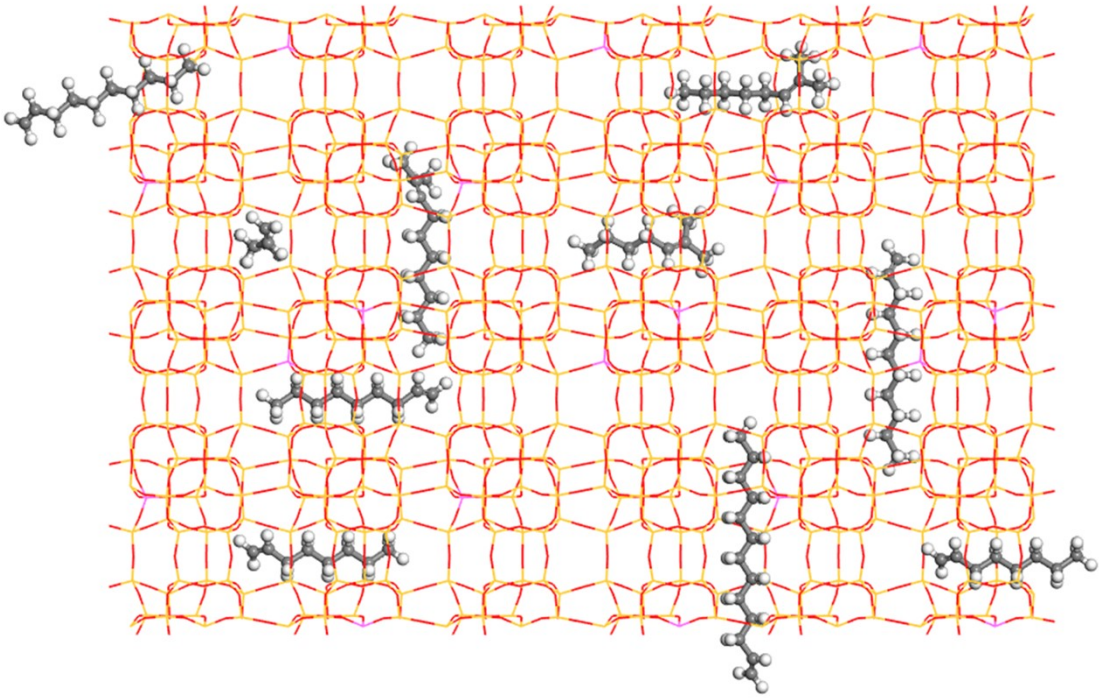

Figure S16. Schematic diagram of the diffusion of olefin molecules in zeolite channels

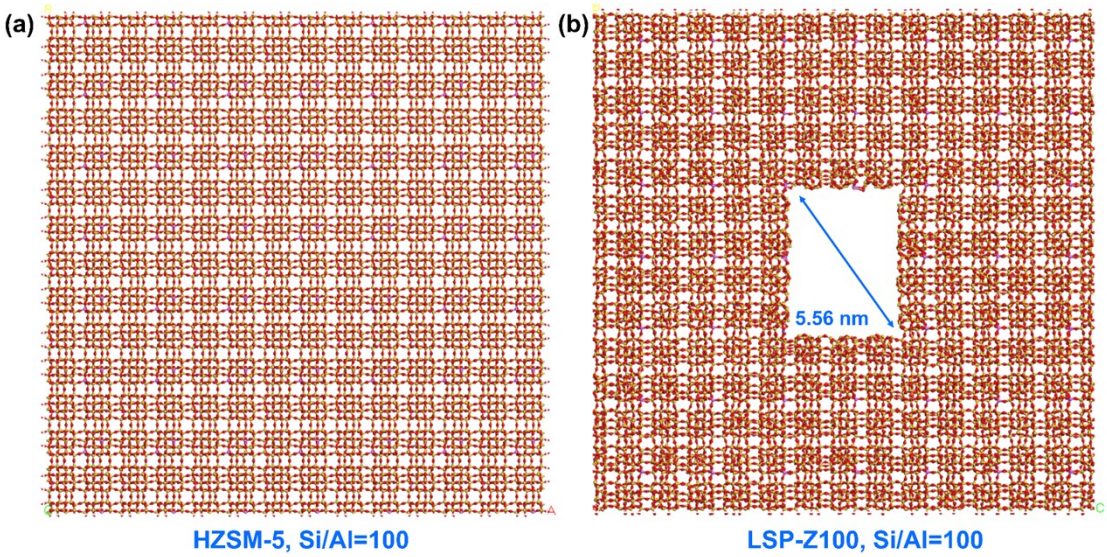

Figure S17. The 7 × 7 × 3 supercell structure with MFI zeolite structure was used to construct (a) HZSM-5 and (b) LSP-Z100 zeolite structures.

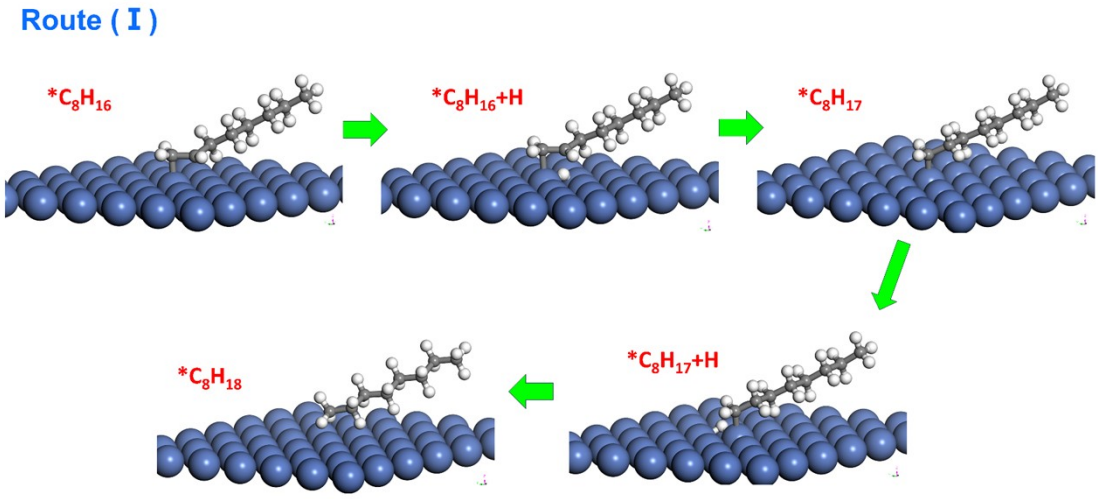

Figure S18. Each step of Route I

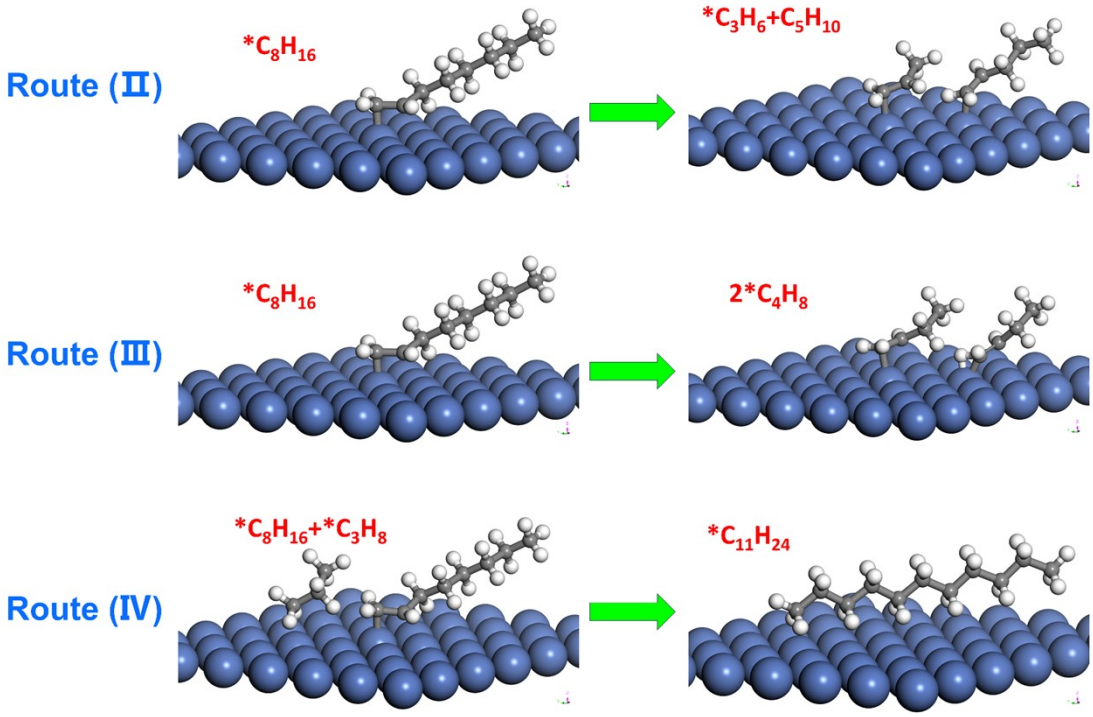

Figure S19. Each step of Route II, III, IV

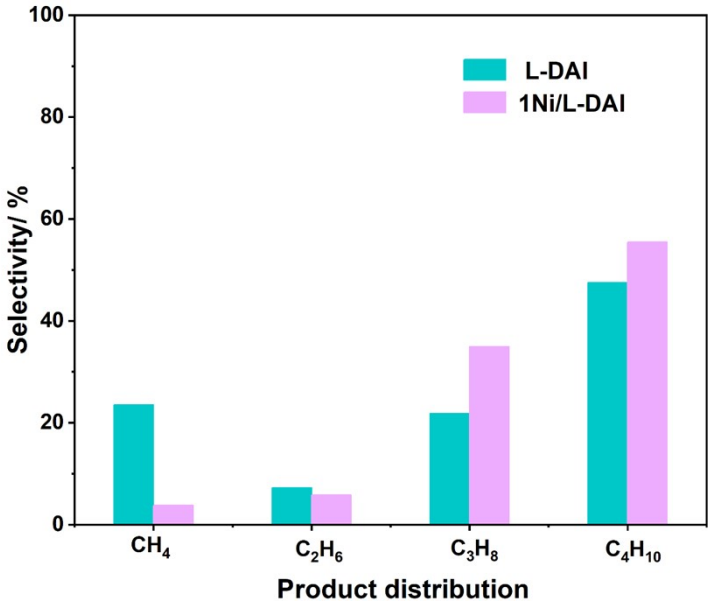

Figure S20. Analysis of C_1–C_4 gaseous products from LDPE hydrocracking catalyzed by L-DAl and 1Ni/L-DAl

Table S1. FWHM of different zeolites in different 2θ

Zeolite	7.86°	8.78°	14.72°	23.12°	23.96°
LSP-Z75	0.2335	0.2777	0.3364	0.3415	0.5949
LSP-Z100	0.223	0.2593	0.3368	0.3231	0.5528
LSP-Z150	0.526	0.6889	1.035	0.7604	0.8927
LSP-Z200	0.4208	0.636	0.8127	0.5657	0.7961
L-DAl	0.19652	0.237	0.2683	0.2892	0.6333
L-DSi	0.2005	0..2566	0.3179	0.31808	0.6035
L-CBr	0.2122	0.2773	0.3339	0.3543	0.5369
L-TBr	0.20895	0.2631	0.3056	0.3387	0.5854
L-TOH	0.2292	0.323	0.5808	0.5411	0.8209
0.5Ni/L-DAl	0.1924	0.2287	0.2779	0.2878	0.4602
1Ni/L-DAl	0.2372	0.2891	0.3608	0.3625	0.63
2Ni/L-DAl	0.1892	0.2275	0.2744	0.3015	0.559
5Ni/L-DAl	0.1848	0.2313	0.2872	0.3152	0.5807

Table S2. Statistics on the particle sizes of Ni nanoclusters in all TEM images of 1Ni/L-DAl shown in Figure S6

Fig	a	b	c	d	e	f	g	h	i	j	k	l	m
Maximum size (nm)	4.7	4.82	5.44	7.42	5.65	7.49	5.29	4.8	5.29	6	5.24	5.3	6.36
Minimum size (nm)	2.28	2.7	2.42	4.28	1.78	1.77	2.98	2.3	3.32	2.88	2.25	3.12	3.09
Average size (nm)	3.6	3.69	3.81	5.7	3.27	4.13	3.73	3.82	4.38	4.27	3.8	4.22	4.18
Overall average size (nm)							4.05						

Table S3. Comparison of physicochemical properties among different zeolites

Catalyst	Si/Al	BET surface area (m^2 g^{-1})	Pore diameter (nm)
HZSM-5	100	412	0.55
HY	100	761	0.76
LSP-Z100	109	508	5.78
Hβ	100	725	0.66
MCM-41	100	984	2.96
TS-1	Si/Ti=100	423	0.57
γ-Al_2O_3	-	279	3.75

Table S4. Comparison of this work with previously reported catalysts in polyolefin hydrocracking performance

Catalyst	Condition	Conversion (%)	Liquid(%)	C_8~C_{12} yield(%)
This work	300℃,1h, 2 Mpa H_2	99	82.15	83.73
Rh−CeO_2/CeHY[1]	300℃,1h, 2 Mpa H_2	99	78.3	76.5
β-Pt@TS-1[2]	250℃,2h, 1 Mpa H_2	99	94	39.6
Ni–W/ZrO_2[3]	250℃,10h, 3 Mpa H_2	99	75.6	25.4
Ni/NbO_x[4]	260℃,5h, 3 Mpa H_2	99	95	46.6
Al-MCM-41[5]	220℃,12h, 2 Mpa H_2	80.62	70.23	C_5~C_{21}:67.5
Pt_n/Hβ[6]	250℃,2h, 2.2 Mpa H_2	99	95	29
5%Ni DSHβ[7]	325℃,1h, 30 bar H_2	95.9	73.9	C_5~C_{12}:61.4
0.5Ni/Beta[8]	280℃,3h, 4MPa H_2	78.4	63.5	C_5~C_{12}:84.8
Ni-WO_3/Al_2O_3-β[9]	280℃,4h, 4MPa H_2	83.8	75.4	46.7
Nb_2O_5-β[10]	240℃,2h, 1MPa H_2	98.2	87.1	57.3
Ru_1-ZrO_2[11]	250℃,8h, 3MPa H_2	97	69	61
Ru/TiO_2-HX[12]	240℃,4h, 2MPa H_2	99	89.4	57.5

Table S5. Diffusion coefficients of olefins in different zeolite channels

Olefins	Ds (10^{-10} m^2/s)	
	HZSM-5	LSP-Z100
n-C_8H_{16}	2.52	6.06
i-C_8H_{16}	3.39	8.03
n-C_9H_{18}	1.91	5.33
i-C_9H_{18}	2.89	5.95
n-$C_{10}H_{20}$	1.06	3.74
i-$C_{10}H_{20}$	1.42	4.62
n-$C_{11}H_{22}$	0.64	1.94
i-$C_{11}H_{22}$	0.91	2.19
n-$C_{13}H_{26}$	0.21	1.48
i-$C_{13}H_{26}$	0.25	1.61

Reference

[1] X Wu, X Liu, et al. A Minimalist Design for a Dual-Catalyst System for High-Efficiency Conversion of Waste Plastics into Liquid Fuel Products. J. Am. Chem. Soc. 2025, 147, 25: 21907–21915.

[2] S Wang, W Wang, et al. Ultra-Narrow Alkane Product Distribution in Polyethylene Waste Hydrocracking by Zeolite Micropore Diffusion Optimization. Angew. Chem. Int. Ed. 2024, e202409288.

[3] C Leng, H Li, et al. Selective hydrocracking of polyolefin waste into branched liquid fuels over a non-noble metal bifunctional Ni–W/ZrO_2 catalyst†. Journal of Materials Chemistry A. 2025, 13, 27546.

[4] X Han, Y Zhou, et al. Hydrogen Spillover-Induced Brønsted Acidity Enables Controllable Hydrocracking of Polyolefin Waste to Liquid Fuels. Angew. Chem. Int. Ed. 2025, 64, e202505518.

[5] Z Wang, L Gao, et al. Accurately tuning the pore size and acidity of mesoporous zeolites for enhancing the catalytic hydrocracking of polypropylene†. Journal of Materials Chemistry A.

[6] S Tian, R Bai, et al. High-Efficiency Hydrocracking of Polyolefin Plastics by Controlling Intimacy between Pt Clusters and Zeolite Acid Sites. J. Am. Chem. Soc. 2025, 147, 30268−30276.

[7] M Azam, A Fernandes, et al. Pore-Structure Engineering of Hierarchical β Zeolites for the Enhanced Hydrocracking of Waste Plastics to Liquid Fuels. ACS Catal. 2024, 14, 16148−16165.

[8] X Han, J Zhang, et al. Engineering noble metal-free nickel catalysts for highly efficient liquid fuel production from waste polyolefins under mild conditions. Fuel, 2025, 382: 133733.

[9] J Sun, C Wu, et al. Noble metal-free tandem catalysis enables efficient upcycling plastic waste into liquid fuel components. Chemical Engineering Journal. 2024, 500: 156988.

[10] S Wang, R Wang, et al. Dual-catalyst system without supported metals toward polyethylene waste upcycling. Journal of Catalysis. 2025, 451: 116383.

[11] J Yan, G Yi, et al. Upcycling polyolefins to methane-free liquid fuel by a Ru1-ZrO_2 catalyst. Nature Communications, (2025) 16:2800.

[12] W Tu, M Chu, et al. SMSI-induced charge transfer for selective hydrogenolysis of polyolefins. Applied Catalysis B: Environmental. 2023, 339: 123122.